



β -Cell Replacement in Mice Using Human Type 1 Diabetes Nuclear Transfer Embryonic Stem Cells

Lina Sui,¹ Nichole Danzl,² Sean R. Campbell,² Ryan Viola,¹ Damian Williams,³ Yuan Xing,⁴ Yong Wang,⁴ Neil Phillips,⁵ Greg Poffenberger,⁵ Bjarki Johannesson,⁶ Jose Oberholzer,⁴ Alvin C. Powers,^{5,7} Rudolph L. Leibel,¹ Xiaojuan Chen,^{2,8} Megan Sykes,^{2,8,9} and Dieter Egli^{1,6}

Diabetes 2018;67:26–35 | <https://doi.org/10.2337/db17-0120>

β -Cells derived from stem cells hold great promise for cell replacement therapy for diabetes. Here we examine the ability of nuclear transfer embryonic stem cells (NT-ESs) derived from a patient with type 1 diabetes to differentiate into β -cells and provide a source of autologous islets for cell replacement. NT-ESs differentiate in vitro with an average efficiency of 55% into C-peptide-positive cells, expressing markers of mature β -cells, including MAFA and NKX6.1. Upon transplantation in immunodeficient mice, grafted cells form vascularized islet-like structures containing MAFA/C-peptide-positive cells. These β -cells adapt insulin secretion to ambient metabolite status and show normal insulin processing. Importantly, NT-ES- β -cells maintain normal blood glucose levels after ablation of the mouse endogenous β -cells. Cystic structures, but no teratomas, were observed in NT-ES- β -cell grafts. Isogenic induced pluripotent stem cell lines showed greater variability in β -cell differentiation. Even though different methods of somatic cell reprogramming result in stem cell lines that are molecularly indistinguishable, full differentiation competence is more common in ES cell lines than in induced pluripotent stem cell lines. These results demonstrate the suitability of NT-ES- β -cells for cell replacement for type 1 diabetes and provide proof of principle for therapeutic cloning combined with cell therapy.

Type 1 diabetes is a disorder characterized by the loss of β -cell mass and function. Because β -cells do not spontaneously regenerate sufficiently to correct diabetes, an exogenous source of β -cells could be useful (1). Transplantation of islets from a pancreatic organ donor can restore physiological regulation of blood glucose in human subjects (2) but require management of allo-immunity. Although autologous cells would not address the recurrence of autoimmunity against transplanted β -cells, it obviates the need to suppress allo-immunity. We have recently shown that pluripotent stem cells matched to a subject with type 1 diabetes can be derived from skin cells by somatic cell nuclear transfer (SCNT) (3). Stem cells can also be derived by induction of pluripotency (4), resulting in highly similar cell types with regard to gene expression and DNA methylation (5). However, the functionality of reprogrammed human stem cells has not been sufficiently tested. Notably, nuclear transfer (NT) from adult cells more consistently results in the production of viable mice (6) than in the production from induced pluripotent stem cells (iPSCs) (7), suggesting that reprogrammed cells derived by SCNT are more often fully differentiation competent (8). Reprogramming by NT recapitulates developmental events that occur upon normal fertilization and allows resetting of the epigenome of the

¹Naomi Berrie Diabetes Center and Department of Pediatrics, College of Physicians and Surgeons, Columbia University Medical Center, New York, NY

²Columbia Center for Translational Immunology, Department of Medicine, College of Physicians and Surgeons, Columbia University Medical Center, New York, NY

³Columbia Stem Cell Core Facility, Columbia University Medical Center, New York, NY

⁴Department of Surgery/Division of Transplantation, University of Illinois at Chicago, Chicago, IL

⁵Division of Diabetes, Endocrinology and Metabolism, Department of Medicine, Vanderbilt University Medical Center, Nashville, TN

⁶New York Stem Cell Foundation Research Institute, New York, NY

⁷VA Tennessee Valley Healthcare System, Nashville, TN

⁸Department of Surgery, College of Physicians and Surgeons, Columbia University Medical Center, New York, NY

⁹Department of Microbiology & Immunology, College of Physicians and Surgeons, Columbia University Medical Center, New York, NY

Corresponding author: Dieter Egli, de2220@cumc.columbia.edu.

Received 28 January 2017 and accepted 14 September 2017.

This article contains Supplementary Data online at <http://diabetes.diabetesjournals.org/lookup/suppl/doi:10.2337/db17-0120/-/DC1>.

Detailed records of data collection and experimentation are available at OSF, osf.io/cdrzs.

Y.X., Y.W., and J.O. are currently affiliated with the Department of Surgery, School of Medicine, University of Virginia, Charlottesville, VA.

© 2017 by the American Diabetes Association. Readers may use this article as long as the work is properly cited, the use is educational and not for profit, and the work is not altered. More information is available at <http://www.diabetesjournals.org/content/license>.

somatic nucleus to an early embryonic state. The generation of iPSCs, in contrast, is performed by ectopic expression of a key set of embryonic transcription factors. Although NT selects for the ability of a cell to advance through embryonic developmental steps, iPSC generation selects for growth in the pluripotent state, not for developmental competence. These differences in the reprogramming process could result in different functional outcomes. However, the differentiation propensities and functional properties of human stem cell lines reprogrammed by SCNT are thus far unknown. The most stringent functional test of human cells is their ability to differentiate into functional β -cells that are able to reverse diabetes in animal models.

Here we assessed whether human pluripotent stem cells derived from skin fibroblasts of a patient with type 1 diabetes by SCNT (1018-NT-ES [embryonic stem] cell) can give rise to differentiated β -cells (1018-NT- β) with qualitative and quantitative physiological performance comparable to naturally occurring β -cells. 1018-NT- β -cells coexpressed C-peptide, pancreatic and duodenal homeobox 1 (PDX1), NK6 homeobox 1 (NKX6.1), as well as musculoaponeurotic fibrosarcoma oncogene family A (MAFA) and showed increased cytosolic calcium and insulin secretion in response to glucose. Upon transplantation, 1018-NT- β -cells protected mice from streptozotocin (STZ)-induced diabetes, and responded to nutrient status by decreasing human C-peptide secretion during fasting and by increasing secretion upon refeeding or glucose administration. In a comparison of NT-ES cell lines and iPSC lines, we found that β -cells could be derived from both cell types, though iPSC lines showed greater variability in differentiation efficiency. Therefore, NT-ES cells matched to a patient with type 1 diabetes could potentially provide a suitable unlimited source of cells for cell replacement to treat diabetes.

RESEARCH DESIGN AND METHODS

Patients and Cell Lines

This study included two human ES (hES) cell lines (INS^{GFP/W} hES and NKX2.1^{GFP/W} hES) (9,10), three NT-ES cell lines (1018-NT-ES, BJ-NT-ES 5, and BJ-NT-ES 6) (3), and seven human iPSC lines (1158-iPSC, 1159-iPSC, 1023-iPSC, 1018-iPSC A and E, and BJ-iPSC M and O) (3). Further information and quality controls regarding these cell lines is provided in Supplementary Table 1. All human subjects research was reviewed and approved by the Columbia University Institutional Review Board and the Columbia University Embryonic Stem Cell Committee. Refer to the Supplementary Data for additional details.

Cell Culture and β -Cell Differentiation

Pluripotent stem cell lines were maintained on mitomycin C-treated primary mouse embryonic fibroblasts (catalog #CF-1 MEF IRR; MTI-GlobalStem) and passaged with TrypLE Express (catalog #12605036; Life Technologies) every 5–7 days. Cells were dissociated with TrypLE Express and plated on Matrigel-coated plates in mTeSR Medium (catalog #05850; STEMCELL Technologies) with 10 μ M Y27632 (catalog #S1049; Selleckchem). Detailed methods and factors used for

differentiation toward β -cells are described in the Supplementary Data. For consistency, β -cell differentiation was performed by one person (L.S.), and comparisons are between differentiation experiments at equal skill levels. All differentiation experiments were included unless a majority of cells died after clustering at the pancreatic progenitor stage. As a quality control for differentiation, part of the cells was stained for stage-specific markers at the definitive endoderm stage, the pancreatic progenitor stage, and the β -cell stage during differentiation.

Static Glucose-Stimulated Insulin Secretion

A total of 10–20 1018-NT- β -cell clusters ($\sim 5 \times 10^5$ cells) and ~ 100 islet equivalent human islets were collected and preincubated in a 500- μ L low-glucose solution for 1 h. Clusters were then sequentially incubated in low-glucose and high-glucose solutions. Incubation in different levels of glucose solutions was repeated once. Supernatants of each condition and protein content were collected and measured using a Mercodia M-Plex ARRAY Chemiluminescent Mercodia Beta Kit. Pictures were taken using a Quansys Q-VIEW Imager and analyzed by Quansys Q-VIEW Software. Refer to the Supplementary Data for additional details.

Dynamic Glucose-Stimulated Insulin Secretion

A microfluidic-based perfusion system was used to determine glucose-stimulated insulin secretion. This experiment was conducted according to previously described methods (11,12). Refer to the Supplementary Data for additional details.

Assessment of Insulin Secretion Response to Other Stimuli

Insulin secretion was evaluated in a cell perfusion apparatus with DMEM containing 0.1% BSA, glucose, and test compounds at a flow rate of 1 mL/min as previously described (13). Refer to the Supplementary Data for additional details.

Immunocytochemistry

Cells at different stages were stained for lineage-specific protein markers during differentiation. Refer to the Supplementary Data for additional details.

Flow Cytometry

The β -cell clusters were dissociated using TrypLE Express into single cells. Cells were fixed with 4% paraformaldehyde for 10 min and followed by permeabilization at -20°C with cold methanol for 10 min. Primary antibodies were added at a dilution of 1:100 in autoMACs Rinsing Solution (catalog #130-091-222; Miltenyi Biotec) containing 0.5% BSA at 4°C for 1 h. Secondary antibodies were added at a dilution of 1:500 at room temperature for 1 h. The cells were filtered with a BD Falcon 12×75 -mm tube with a cell strainer cap (catalog #352235; BD Biosciences) and subsequently analyzed by flow cytometer. Data were analyzed using FlowJo software. Negative controls were performed by only adding secondary antibodies.

Calcium Imaging

Ca²⁺ imaging was used to determine the effect of high glucose concentrations on changes in intracellular Ca²⁺.

Imaging using Fura-2AM (Thermo Fisher Scientific, Waltham, MA) was carried out using on a Nikon Eclipse TE 3500 Inverted Microscope equipped with a $\times 40$ 1.30 numerical aperture objective (Nikon USA, Melville, NY), a pco.EDGE CMOS camera (PCO AG, Kelheim, Germany), a Lambda LS light source, a Lambda LS-2 filter wheel with 340/26-nm BP (band pass) and 387/11-nm BP excitation, a 409-nm LP (long pass) dichroic, and 510/84-nm emission filters (all from Sutter Instruments, Novato, CA). Refer to the Supplementary Data for additional details.

Transplantation and In Vivo Assay

Eight- to 10-week-old male and female immunocompromised mice (NOD.Cg-Prkdcscid Il2rgtm1Wjl/SzJ [NSG] mice; catalog #005557; The Jackson Laboratory) were used for transplantation. For subcutaneous space transplantation, 40–100 clusters (1–2 million cells with on average 55% C-peptide-positive cells) were collected and settled in a tube with 50- μ L of differentiation medium. These clusters were transferred onto gelfoam prewetted with differentiation medium. The clusters and gelfoam were overlaid with 20 μ L of Matrigel. The resultant implant constructs were placed in a cell incubator for 5 min and then prewarmed medium were added for further culture until implantation (14,15). All animal protocols were approved by the Institutional Animal Care and Use Committee in Columbia University. Refer to the Supplementary Data for additional details.

Statistical Analysis

Data were analyzed by unpaired *t* test and by one-way ANOVA followed by Tukey's multiple-comparison test (GraphPad Prism 6; GraphPad Software, Inc., La Jolla, CA) and expressed as mean \pm SD. The differences observed were considered statistically significant at the 5% level and were displayed on the figures as follows: **P* < 0.05, ***P* < 0.01, ****P* < 0.001, *****P* < 0.0001.

RESULTS

An Efficient Protocol for the Derivation of Monohormonal C-Peptide-Positive Cells

We optimized the protocol based on two recently published protocols (16,17) using INS^{GFP/W}-hES cells (9). In particular, we tested the induction of pancreatic progenitors expressing both PDX1 and NKX6.1, which are required for the development of mature β -cells (18). Induction of definitive endoderm in a monolayer culture by the STEMdiff Definitive Endoderm Kit resulted in $\geq 95\%$ definitive endoderm cells expressing SOX17, FOXA2, CXCR4, and C-kit on day 4 (Supplementary Fig. 1A and B). For further differentiation, we applied compounds individually, or in combination, including bone morphogenetic protein 4 (BMP4) inhibitor LDN193189 (LDN), fibroblast growth factor 10, BMP4, epidermal growth factor (EGF), resulting in activation of protein kinase C, TPB (an activator of protein kinase C), sonic hedgehog inhibitor KAAD-cyclopamine (Cyclo), and retinoid acid, which have all been reported to induce pancreatic

progenitors (14,16,17,19,20). We found that adding EGF for 3 days after 2 days of treatment with Cyclo, LDN, and retinoic acid was the most efficient, with $\sim 30\%$ of cells expressing both PDX1 and NKX6.1 in experiments performed at 80% plating density and in a 96-well plate (Supplementary Fig. 1C). Increasing the plating density of ES cells to 100% and differentiation in a 6-well plate led to a further increase ($\sim 70\%$ PDX1- and NKX6.1-positive cells can be routinely obtained after adding EGF for 3 days) (Supplementary Fig. 1D). LDN was omitted during treatment with EGF, because it resulted in the premature induction of NGN3-positive cells (Supplementary Fig. 1E), which is consistent with previous observations that LDN inhibition of BMP4 signaling induces the expression of NGN3 (21).

We then applied a 3D culture by aggregating the cells in low attachment plates from the pancreatic progenitor stage until the β -cell stage using factors reported in a recently published protocol (Fig. 1A) (17). Although a monolayer culture also resulted in C-peptide-positive cells ($\sim 7\%$), the 3D culture enabled the generation of much greater numbers of C-peptide-positive cells ($> 50\%$) (Supplementary Fig. 2A). Of these, the majority (70%) were monohormonal, which is shown by the coexpression of NKX6.1 and C-peptide and the absence of glucagon. We also observed that 11% of cells coexpressed C-peptide and glucagon (Supplementary Fig. 2A and B).

Efficient Differentiation of β -Cells From 1018-NT-ES Cells

Using our optimized protocol, we assessed the ability of NT-ES cells to differentiate into C-peptide-positive cells (Fig. 1A). Differentiation of 1018-NT-ES cells resulted in the generation of $\sim 95\%$ SOX17- and FOXA2-positive definitive endoderm cells (Fig. 1B and C), $\sim 97\%$ PDX1-positive cells, and $\sim 80\%$ PDX1 and NKX6.1 coexpressing cells at the pancreatic progenitor stage (Fig. 1D and E). At the β -cell stage, on day 27 of differentiation, $\sim 80\%$ of cells in the clusters were PDX1 positive, and up to $\sim 77\%$, and on average $\sim 55\%$, of the cells were C-peptide positive ($n = 5$) (Fig. 1F and L). Among the C-peptide-positive cells, $\sim 50\%$ coexpressed the β -cell marker NKX6.1 (Fig. 1G and L) as well as MAFA (Fig. 1H and L), and they were monohormonal and did not coexpress the other endocrine hormones glucagon or somatostatin (Fig. 1I, K, and L). The efficient differentiation toward β -cells was also apparent at the mRNA level. Quantitative RT-PCR revealed the absence of *OCT4* expression and the upregulation of genes expressed in the pancreatic endocrine lineage: *PDX1*, *FOXA2*, *NGN3*, *NKX6.1*, *SUR1*, *INS*, and *GLU* (Supplementary Fig. 3A and Supplementary Table 2). Insulin and *MAFA* expression was lower in 1018-NT- β -cells, although the differences were not significant because of the variation in human islets. Glucagon and *NGN3* expression were higher in 1018-NT- β -cell clusters than in human islets, indicating ongoing maturation from endocrine progenitors (Supplementary Fig. 3B). A total of 2% of C-peptide-positive cells were proliferating, as indicated by the expression of Ki67 (Fig. 1J). Taken

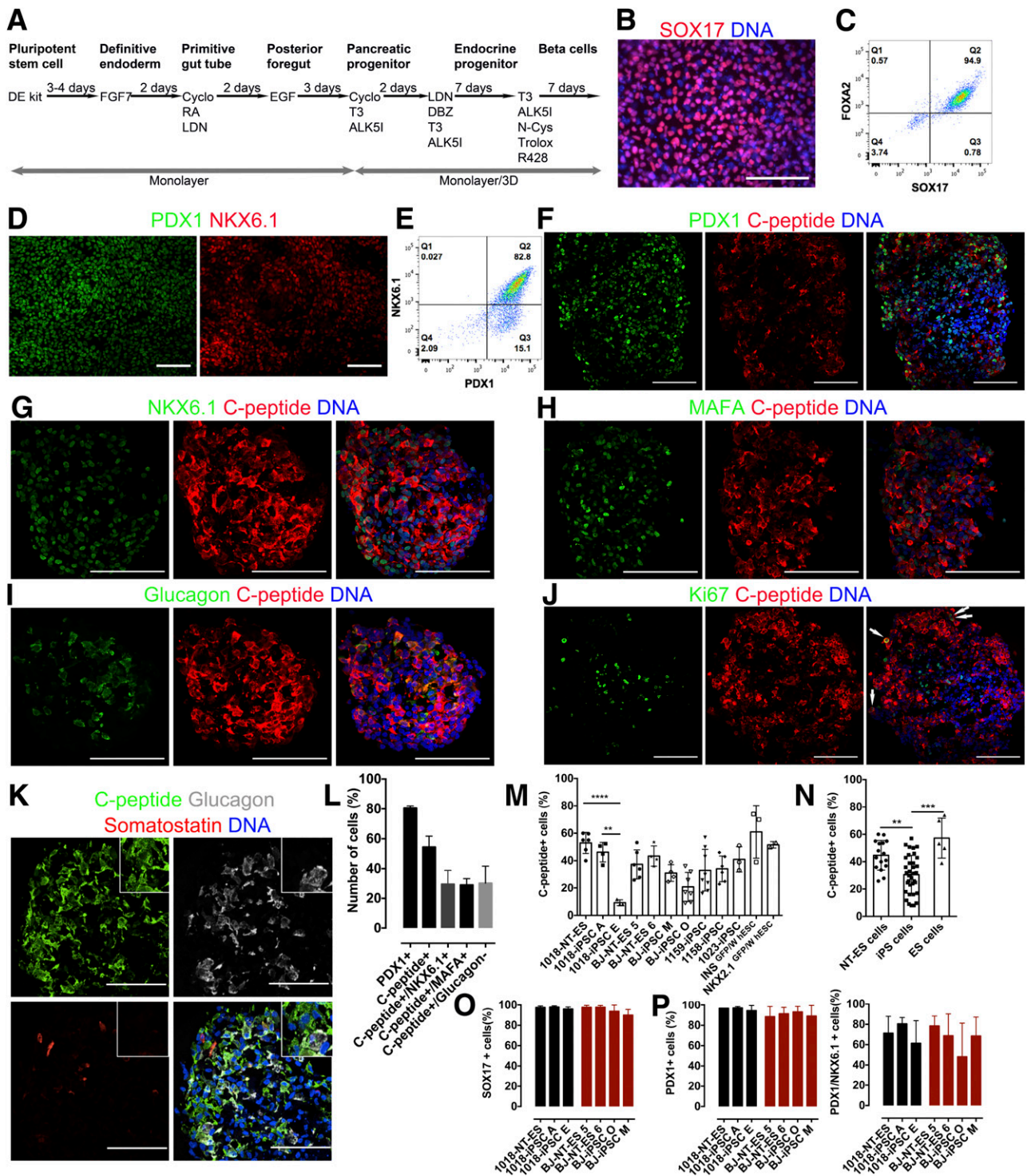


Figure 1—Efficient generation of 1018-NT-β-cells from 1018-NT-ES cells. **A**: Schematic of the protocol used for β-cell differentiation. Immunostaining (**B**) and quantification (**C**) of SOX17-positive cells at the definitive endoderm stage by flow cytometry. Immunostaining (**D**) and quantification (**E**) of PDX1- and NKX6.1-positive cells at the pancreatic progenitor stage by flow cytometry. **F–K**: Immunostaining analysis of pancreatic specific protein expression of 1018-NT-β-cell clusters using confocal microscopy. Scale bars, 100 μm. Arrows in panel **J** indicate Ki67-positive proliferating C-peptide-positive cells. **L**: Quantification of cells positive for PDX1, C-peptide, C-peptide and NKX6.1, and C-peptide and MAFA, and cells positive for C-peptide but negative for glucagon in 1018-NT-β-cell clusters. **M** and **N**: Quantification of C-peptide-positive cells differentiated from indicated cell lines. **O**: Quantification of SOX17-positive cells at definitive endoderm stage derived from 1018-NT-ES ($n = 3$), 1018-iPSC A ($n = 3$), 1018-iPSC E ($n = 2$), BJ-NT-ES 5 ($n = 2$), BJ-NT-ES 6 ($n = 2$), BJ-iPSC O ($n = 3$), and BJ-iPSC M ($n = 2$) cell lines. **P**: Quantification of PDX1-positive cells and PDX1- and NKX6.1-positive cells at pancreatic progenitor stage derived from 1018-NT-ES ($n = 3$), 1018-iPSC A ($n = 2$), 1018-iPSC E ($n = 3$), BJ-NT-ES 5 ($n = 7$), BJ-NT-ES 6 ($n = 4$), BJ-iPSC O ($n = 4$), and BJ-iPSC M ($n = 4$) cell lines. ** $P < 0.01$; *** $P < 0.001$; **** $P < 0.0001$.

together, these data show that islet-like clusters of endocrine cells, including C-peptide-, NKX6.1-, and MAFA-positive monohormonal β -cells can be efficiently derived from the NT-ES cells of a patient with type 1 diabetes.

We also compared the efficiency of differentiation into C-peptide-positive cells among different cell lines. We used two type 1 diabetes iPSC lines (1018-iPSC A and 1018-iPSC E) that are isogenic to the type 1 diabetes NT-ES cell line (1018-NT-ES) as well as two healthy control iPSC lines (BJ-iPSC M and BJ-iPSC O) with isogenic NT-ES cell lines (BJ-NT-ES 5 and BJ-NT-ES 6). We also studied two hES cell lines (INS^{GFP/W} hESC and NKX2.1^{GFP/W} hESC), another iPSC line derived from a patient with type 1 diabetes (1158-iPSC), as well as two iPSC lines from healthy subjects (1159-iPSC and 1023-iPSC) (Supplementary Table 1). We found that the percentages of C-peptide-positive cells derived from 1018-NT-ES and BJ-NT-ES cell lines were comparable to those obtained from the two hES cell lines (Fig. 1M). The number of C-peptide-positive cells derived from 1018-iPSC E was significantly lower than that in the isogenic 1018-NT-ES cell line and was also decreased in the BJ-iPSC O compared with that of isogenic BJ-NT-ES cell lines, although it is not statistically significant because of the great variability between individual experiment in BJ-iPSC O (Fig. 1M). iPSC lines derived from different subjects showed greater variability as well (8–57%) (Fig. 1M and N) and, on average, a lower capacity to differentiate to C-peptide-positive cells (Fig. 1N). To determine the time point at which these differences arise, we quantified the percentage of SOX17-positive cells at the definitive endoderm and PDX1- and NKX6.1-positive cells at the pancreatic progenitor stage. We found efficient differentiation to SOX17- and to PDX1-positive cells in all seven cell lines tested (Fig. 1O and P). Therefore, differentiation of iPSCs is compromised primarily during the transition from pancreatic progenitors to β -cells.

1018-NT- β -Cell Clusters Secrete Insulin in Response to Physiological Stimuli

To evaluate the functional properties of 1018-NT- β -cell clusters, we first compared hormone production with human islets. The insulin and C-peptide content of 1018-NT- β -cell clusters was approximately sixfold lower than in human islets (Fig. 2A and B). The ratio of proinsulin to insulin was elevated in 1018-NT- β -cells, though not statistically significant (Fig. 2D and E). We then compared the hormone secretion in a low-glucose medium. 1018-NT- β -cell clusters secreted 21-fold less insulin than human islets, whereas C-peptide secretion was reduced 9-fold (Fig. 2F and G). In contrast, the secretion of proinsulin was comparable to human islets, resulting in a high ratio of proinsulin to insulin in 1018-NT- β -cells (Fig. 2I and J). The production of glucagon showed no significant difference between 1018-NT- β -cell clusters and human islets, whereas the secretion was moderately higher in human islets compared with 1018-NT- β -cell clusters (Fig. 2C and H).

To study glucose-stimulated insulin secretion, we exposed 1018-NT- β -cell clusters to different concentrations

of glucose and other secretagogues in both a static assay and a perfusion assay. Sequential glucose challenge resulted in a modest increase of insulin secretion (Fig. 2K). The fold increase in secretion was comparable to that of human islet preparations, though the quality of available human islets was not optimal (16). In a cell monolayer consisting of 50% C-peptide-positive cells (Supplementary Fig. 4A), the cytosolic calcium signal increased in response to glucose stimulation in 20% of single cells measured (Fig. 2L) and also increased at the population level ($n = 2$) (Supplementary Fig. 4B and C). The amplitude of the response was lower than that in human islets (17). A much greater increase of cytosolic calcium was observed in response to potassium (Fig. 2L). Consistent with a modest increase in cytosolic calcium, a modest increase in insulin secretion occurred in a perfusion assay in response to glucose stimulation (Fig. 2M). However, the magnitude of the response was not consistent across different cell preparations (Fig. 2N). Unlike their muted response to glucose, 1018-NT- β -cell clusters showed increased insulin secretion in response to various other stimuli, including isobutylmethylxanthine, tolbutamide, L-arginine, and KCl (Fig. 2M and N). Dithizone staining confirmed that 1018-NT- β -cell clusters contained high levels of zinc ($n = 2$) (Fig. 2O), and electron microscopy detected crystallized mature insulin granules (Fig. 2P), similar to human islets (Fig. 2Q). A few cells also showed mixed endocrine granules (Supplementary Fig. 4D), which is consistent with the persistence of double hormone-positive cells (Fig. 1J). These functional tests of 1018-NT- β -cells show that despite sharing key features with primary β -cells, functional differences remain in vitro, including reduced insulin content, reduced processing of insulin, and a reduced ability to secrete insulin in response to glucose.

1018-NT- β -Cell Clusters Maintain Normal Blood Glucose Level in Mice With STZ-Induced Diabetes

To determine whether maturation to fully mature β -cells occurred in vivo, we transplanted 1018-NT- β -cell clusters containing 1–2 million cells subcutaneously into immunodeficient mice ($n = 22$) (14,15). Seven batches of 1018-NT- β -cell clusters were prepared independently for transplantation. The percentage of C-peptide-positive cells in clusters used for engraftment ranged from 40% to 77%. Because the skin is not a widely used location for the grafting of pancreatic β -cells, we first examined cell survival on day 7 after transplantation ($n = 1$). C-peptide-positive clusters were detected in the graft (Supplementary Fig. 6A). Only a few C-peptide-positive cells were undergoing apoptosis, as indicated by TUNEL staining (Supplementary Fig. 6B). Therefore, subcutaneous transplantation is compatible with viable 1018-NT- β -cells.

Human C-peptide was detected at low levels in mouse serum as early as 1 week after transplantation and increased gradually thereafter. At 1 week after grafting, ~2% of 1018-NT- β -cells were proliferating based on Ki67 staining (Supplementary Fig. 6C). Mice that remained human C-peptide negative were sacrificed, and no graft was

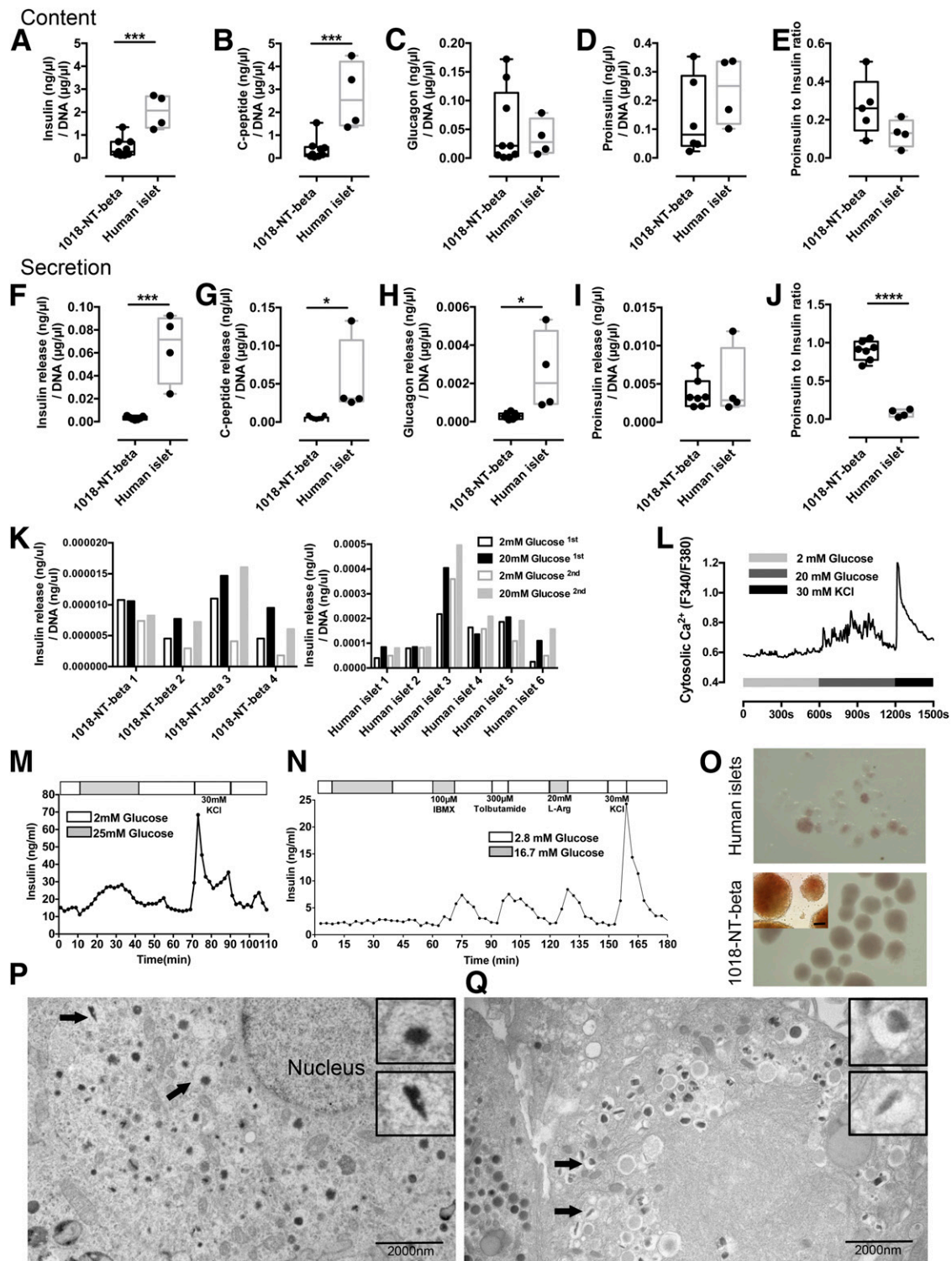


Figure 2—1018-NT-β-cell clusters show similarities and differences with pancreatic β-cells in vitro. **A–E**: Comparison of insulin, C-peptide, glucagon, proinsulin production, and proinsulin-to-insulin ratio between 1018-NT-β-cell clusters (1018-NT-β) ($n = 6$ for proinsulin; $n = 9$ for C-peptide, glucagon, and insulin) and human islets ($n = 4$). **F–J**: Insulin, C-peptide, glucagon, proinsulin secretion, and proinsulin-to-insulin ratio upon 2 mmol/L glucose incubation for 30 min were compared between 1018-NT-β-cell clusters ($n = 7$) and human islets ($n = 4$). **K**: Static insulin secretion assay in response to the multiple challenges with 30 min of 2 and 20 mmol/L glucose on 1018-NT-β ($n = 4$ different batches) and human islet ($n = 6$ different batches). **L**: Cytosolic calcium influx signals in response to 2 mmol/L glucose, 20 mmol/L glucose, and 30 mmol/L KCl at single cell level. Insulin secretion in response to a dynamic glucose challenge and KCl challenge using a microfluidic-based perfusion system (**M**) and other stimuli, including isobutylmethylxanthine, tolbutamide, and L-arginine, in another cell perfusion apparatus (**N**). **O**: Dithizone staining of human islets and 1018-NT-β-cell clusters. Inset with size bar (100 μm). Electron microscopy of 1018-NT-β-cells (**P**) and human islets (**Q**). Representative insulin granules are indicated by black arrows and magnified. * $P < 0.05$; *** $P < 0.001$; **** $P < 0.0001$.

found (Supplementary Fig. 5A). Of the 22 mice, 16 were successfully grafted, with detectable C-peptide secretion. Mice transplanted with 1,000 islet equivalent human islets from four preparations under the kidney capsule all secreted human C-peptide ($n = 7$) (Supplementary Fig. 5B). Approximately 3 months after transplantation, nine mice from four batches of cell preparation were fasted for 13 h, and the blood glucose and human C-peptide levels were measured before and 3 h after refeeding. Human C-peptide serum levels were increased in eight of nine mice after refeeding, concurrent with an increase in blood glucose levels, indicating that the grafted 1018-NT- β -cells were metabolically responsive (Fig. 3A and B). The circulating concentrations of human insulin and proinsulin were also measured after 13 h of fasting, and the ratio was comparable to those obtained in mice transplanted with human islets under the kidney capsule (Fig. 3C). Mice achieving serum human C-peptide concentrations >100 pmol/L ($n = 11$) were treated with STZ to specifically ablate endogenous mouse β -cells while leaving the transplanted human β -cells intact. Successful ablation was demonstrated in 10 of 11 mice by either mouse C-peptide ELISA ($n = 9$) (Fig. 3D) or immunostaining of mouse glucagon and C-peptide in pancreata ($n = 2$) (Supplementary Fig. 5E). A single mouse with remaining mouse

C-peptide (STZ-9) was excluded from further analysis. Of the 10 mice with successful mouse β -cell ablation, 9 maintained normal blood glucose levels, whereas all 3 mice without grafted cells failed to control their blood glucose levels (Fig. 3E). To evaluate the response of 1018-NT- β -cell grafts to varying blood glucose concentrations, we fasted mice for 13 h followed by glucose injection. Serum human C-peptide levels decreased with blood glucose during fasting and increased more than twofold after the injection of glucose at either 30 or 60 min (Fig. 3F and Supplementary Fig. 5C). The 1018-NT- β -cell-grafted mice showed clearance of blood glucose at rates comparable to that of mice transplanted with human islets (Fig. 3G and Supplementary Fig. 5D). Nontransplanted STZ-treated mice failed to clear glucose from the circulation. To determine whether blood glucose was regulated by 1018-NT- β -cells, grafts were surgically removed in two mice. An immediate rise in blood glucose levels was observed (Fig. 3H). Therefore, 1018-NT- β -cell clusters are responsive to the metabolic state of recipient mice and are adequate for homeostatic regulation of mouse blood glucose levels.

To determine the morphology and composition of the grafts, we sacrificed the mice and performed immunocytochemistry and histology. All examined grafts were contained in the gelfoam scaffold, remained at the site of transplantation and showed no

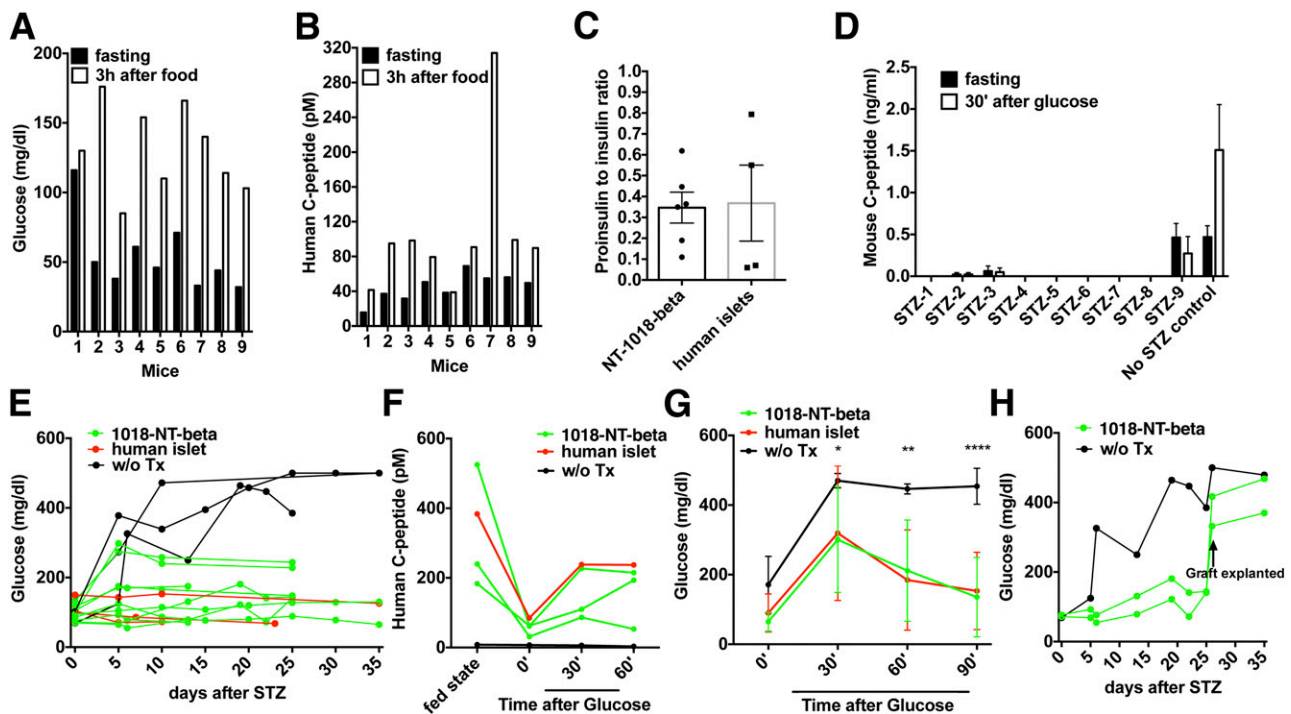


Figure 3—1018-NT- β -cell clusters protect mice from STZ-induced diabetes. *A* and *B*: Blood glucose and human C-peptide serum concentration in mice at ~ 3 months after transplantation with 1018-NT- β -cell clusters at fasting and 3 h after refeeding (after food) ($n = 9$). *C*: Serum human proinsulin-to-insulin ratios of 1018-NT- β -cell clusters and human islets after 3 months of transplantation. (Each black dot or square indicates an individual mouse grafted with indicated cells.) *D*: Mouse C-peptide levels at 2 weeks after STZ treatment before and after glucose injection. *E*: Blood glucose levels of STZ-treated mice without transplantation (w/o Tx) ($n = 3$) and transplanted with 1018-NT- β -cell clusters (1018-NT- β) ($n = 8$) and with human islets ($n = 3$). *F*: Serum human C-peptide concentrations of STZ-treated mice at fasting and at 30 and 60 min after intraperitoneal glucose injection. *G*: Glucose tolerance test of STZ-treated mice without transplantation ($n = 4$) and transplanted with 1018-NT- β -cell clusters ($n = 8$) and with human islets ($n = 3$) in the fed state, the fasting state, and 30–90 min after glucose injection. *H*: Blood glucose levels of STZ-treated mice before and after grafts were removed ($n = 2$). * $P < 0.05$; ** $P < 0.01$; **** $P < 0.0001$.

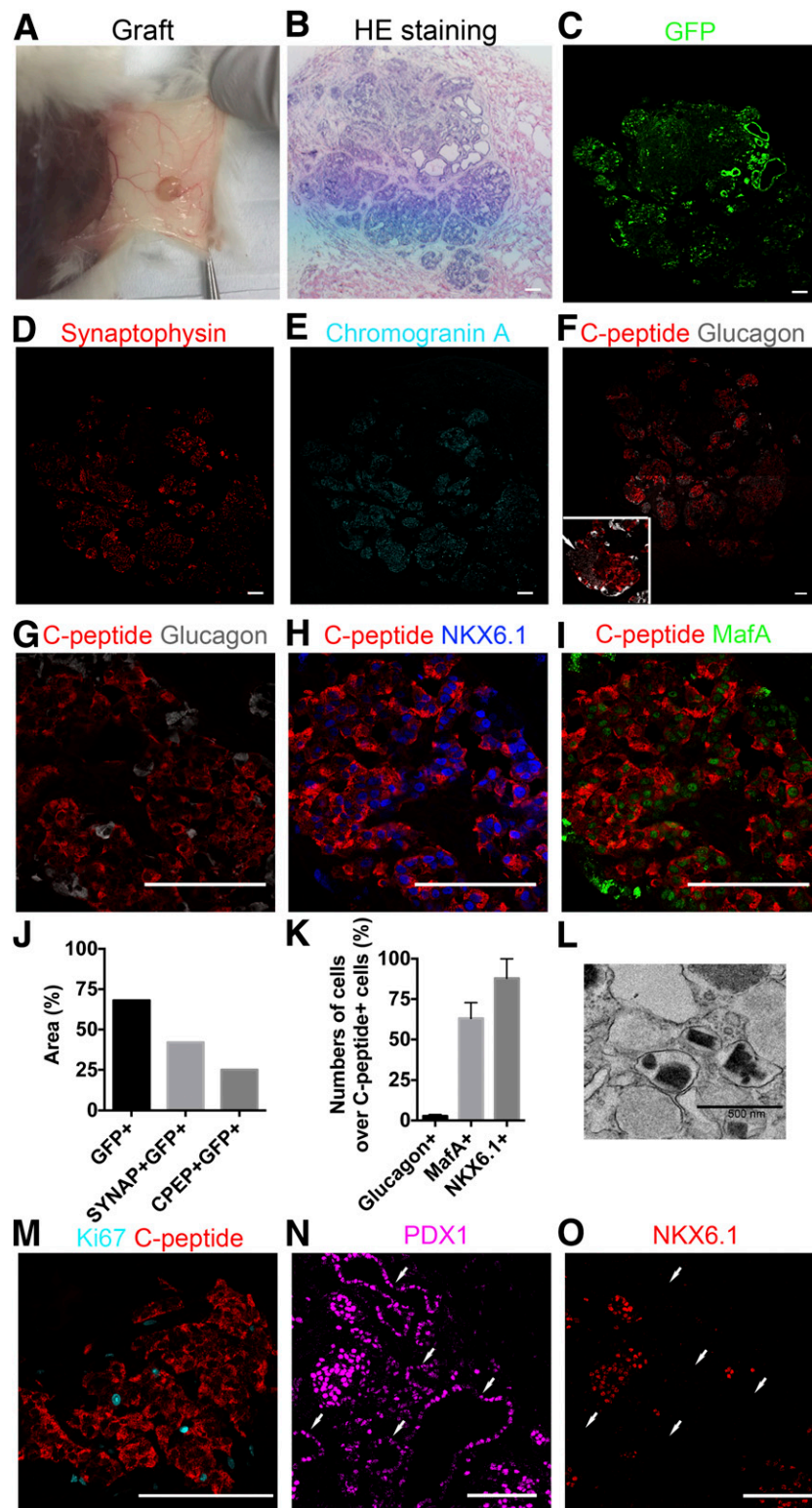


Figure 4—1018-NT- β -cell clusters contain mature endocrine cells in vivo. *A*: Graft morphology under the skin before excision at 5 months after transplantation. *B*: Hematoxylin-eosin (HE) staining of a graft under frozen sections. *C–I*: Immunostaining for indicated proteins. Inset in *F* indicates a blood vessel containing blood cells (arrow). *J*: Quantification of the positive area for indicated marker. GFP-positive area indicates all human cells, synaptophysin (SYNAP)-positive area indicates endocrine cells and C-peptide (CPEP)-positive area indicates β -cells. *K*: Quantification of C-peptide-positive cells coexpressing glucagon, MAFA, and NKX6.1. *L*: Electron microscopy showing representative mature insulin granules in grafted cells. *M*: Immunostaining for C-peptide and Ki67 in grafted cells. *N*: Immunostaining of ductal structures for PDX1 and NKX6.1 in the graft. Scale bars for *B–I* and *M–O*, 100 μ m.

signs of overgrowth (Fig. 4A and B). Because we had marked the 1018-NT-ES cells with a constitutively expressed GFP transgene, we could distinguish mouse cells from human cells based on GFP fluorescence (Fig. 4C). Grafts consisted predominantly of GFP-positive human cells (68% of total grafted area), expressing synaptophysin (42% of the synaptophysin-positive/GFP-positive area of total grafted area), chromogranin A and C-peptide (25% of the C-peptide-positive/GFP-positive area of the total grafted area) (Fig. 4D–F, and J). Glucagon-positive cells encircled the periphery of C-peptide-positive cell clusters or were mingled within clusters of C-peptide-positive cells (Fig. 4F and G and Supplementary Fig. 6D), with the latter pattern resembling human islets (22). Vascularization was also observed in islets indicated by the blood cells (Fig. 4F). In contrast to *in vitro* cultures and at 1 week after transplantation (Supplementary Fig. 6A), in which up to half of the C-peptide-positive cells also contained glucagon (Fig. 1L), double hormone-positive cells were rare *in vivo* 20 weeks after transplantation (<3%; Fig. 4G and K). Grafts were positive for C-peptide, NKX6.1, and MAFA (Fig. 4H and I). Eighty-eight percent of C-peptide-positive cells expressed NKX6.1, and 63% of them coexpressed MAFA (Fig. 4K), which is similar to the human pancreas (23). Electron microscopy of the grafted cells further confirmed the presence of β -cell granules (Fig. 4L). We also observed that 3% C-peptide-positive cells were proliferating, as indicated by the coexpression of Ki67 (Fig. 4M). Besides endocrine tissue, we also found pancreatic ductal structures that express only PDX1 but not NKX6.1 (Fig. 4N and O). Three of 11 examined grafts gave rise to cystic structures, but no teratoma-like growths were found (Supplementary Fig. 6E). Cystic structures were composed of CK19-positive cells that did not coexpress PDX1 (Supplementary Fig. 6F and G), suggesting that they are of endodermal origin. These results show that 1018-NT-ES-derived C-peptide-positive cells mature to fully functional β -cells *in vivo*.

DISCUSSION

Here we show that pluripotent stem cells created by SCNT from an individual with long-standing type 1 diabetes can efficiently give rise to physiologically competent β -cells that are sufficient for metabolic homeostasis upon transplantation into mice lacking endogenous β -cells. These results provide a proof of concept for the use of therapeutic “cloning”: NT-mediated reprogramming combined with autologous cell therapy (24,25).

To efficiently derive β -cells from pluripotent stem cells, we used EGF signaling to induce the generation of NKX6.1-positive cells at the pancreatic progenitor stage, which is consistent with a recently published report (20). Although the 1018-NT- β -cells expressed markers of mature pancreatic β -cells, a number of differences with human islets were noted *in vitro*. 1018-NT- β -cells showed proliferation rates comparable to those of human β -cells in the prenatal (17–32 weeks of gestation) pancreas (26). 1018-NT- β -cells synthesized and secreted less insulin and showed an elevated ratio of proinsulin to insulin. Furthermore, 1018-NT- β -cells

showed only a modest increase in cytosolic calcium and a modest increase in insulin secretion in response to high glucose concentrations. These results are consistent with previous observations in hES cell-derived β -cells (16,17) and are characteristic of human fetal islets (27–29). Therefore, this suggests that the differences of 1018-NT- β -cells with pancreatic β -cells represent an earlier developmental stage of differentiation. However, within 2 months after transplantation into mice, no differences to human islets were observed. 1018-NT- β -cell grafts responded to meals and intraperitoneal glucose with the release of insulin. The ratio of serum human proinsulin to insulin was comparable to that of human islets, indicating normal processing. Importantly, we found that the 1018-NT- β -cells could maintain normal blood glucose concentrations in mice lacking native β -cells.

Surprisingly, we found that though both iPSCs and ES cells were able to differentiate to C-peptide-positive cells, iPSCs were more variable in their differentiation efficiency. β -Cells differentiated from iPSCs from subjects with type 1 diabetes were reported previously (4,30), but a comparison of differentiation efficiencies was not a topic of these studies. Our observations are consistent with previous reports demonstrating that some iPSC lines are refractory to differentiation and cell maturation, whereas others differentiate with an efficiency similar to ES cells (31). The underlying molecular reasons for these differences in efficiency compared with β -cells are not currently understood and may require molecular analysis in cells at various stages of differentiation rather than in undifferentiated stem cells alone, which show similar molecular profiles (5).

In summary, our results demonstrate that SCNT provides patient-specific cell lines that can be efficiently differentiated to C-peptide-positive cells. When transplanted into mice, these cells formed islet-like structures and showed metabolic phenotypes consistent with their nominal cellular identities. Therefore, NT-ES cells hold great promise for autologous cell replacement for diabetes. Future studies will focus on improving graft function, for example by the addition of autologous vascularized cells (32). Furthermore, these NT-ES- β -cells provide a tool with which to study the interactions of elements of the type 1 diabetes immune system reconstituted from patient bone marrow (33) with type 1 diabetes-derived β -cells from the same subject.

Acknowledgments. The authors thank Dr. Claudia Doege (Naomi Berrie Diabetes Center, College of Physicians and Surgeons, Columbia University Medical Center) and Dr. Fabrizio Barbetti (Clinical Biochemistry and Molecular Biology, Department of Experimental Medicine and Surgery, University of Rome Tor Vergata) for critical reading of the manuscript. The authors also thank Dr. Robin S. Goland (Naomi Berrie Diabetes Center, College of Physicians and Surgeons, Columbia University Medical Center) for helpful discussions. In addition, the authors thank the Columbia Nano Initiative (CNI) for the use of its shared facilities and the Fu Foundation School of Engineering and Applied Science and the Faculty of Arts & Sciences, Columbia University, for their support of the CNI Facilities.

Funding. This research was supported by the Russell Berrie Foundation Program in Cellular Therapies for Diabetes, New York State Stem Cell Science (NYSTEM) IDEA award C029552, the Leona and Harry Helmsley Charitable Trust (grant

2015PG-T1D069), Human Islet Research Network grant UC4-DK-104207, The National Institute of Diabetes and Digestive and Kidney Diseases/National Institutes of Health (NIH) grant R01-DK-103585 for the iPSC aspects of the work, American Diabetes Association Fellowship Award 7-11-MN-62, the JDRF Microfluidic-Based Functional Facility at University of Illinois Chicago under NIH grant R01-DK-091526 (J.O.) and the Chicago Diabetes Project, and the New York Stem Cell Foundation. Work in the Powers group was supported by the NIH (grants DK-72473, DK-89572, DK-104211, and DK-106755), the JDRF, the Department of Veterans Affairs, and the Vanderbilt Diabetes Research and Training Center (grant DK-20593). These studies used the resources of the Diabetes and Endocrinology Research Center Flow Core Facility, which was funded in part through Diabetes and Endocrinology Research Center grant 5P30-DK-063608. INSGFP/W-hES cells were a gift from Dr. Edouard G. Stanley, and NKX2.1GFP/W-hES cells were a gift from Dr. Andrew G. Elefanti. Research reported in this publication was performed in the CCTI Flow Cytometry Core, which is supported in part by the Office of the Director, NIH, under awards S10-RR-027050 and S10-OD-020056. L.S. is a Berrie Foundation Scholar. D.E. is a New York Stem Cell Foundation-Robertson Investigator.

Duality of Interest. No potential conflicts of interest relevant to this article were reported.

Author Contributions. L.S. designed the studies, performed differentiation of all cell lines and downstream experiments, analyzed the data, and wrote the manuscript with input from all authors. N.D. performed transplantation of human islets under the kidney capsule. S.R.C. performed transplantation of human islets under the kidney capsule and provided human islets. R.V. assisted with the cell culture. D.W. performed calcium imaging. Y.X., Y.W., and J.O. performed microfluidic perfusion and data analysis. N.P. and G.P. performed and analyzed the perfusion data. B.J. derived iPSC-1158 and -1159 cell lines. A.C.P., R.L.L., and M.S. provided guidance in the design and interpretation of studies. X.C. provided human islets and guidance in the design and interpretation of the studies. D.E. provided guidance in the design and interpretation of the studies, designed the studies, discussed the results, and reviewed and edited the manuscript. D.E. is the guarantor of this work and, as such, had full access to all the data in the study and takes responsibility for the integrity of the data and the accuracy of the data analysis.

Prior Presentation. Parts of this study were presented at the 8th Network for Pancreatic Organ Donor with Diabetes (nPOD) Annual Meeting, Miami, FL, 21–24 February 2016, and at the 15th International Society For Stem Cell Research (ISSCR) Annual Meeting, Boston, MA, 14–17 June 2017.

References

- Johannesson B, Sui L, Freytes DO, Creusot RJ, Egli D. Toward beta cell replacement for diabetes. *EMBO J* 2015;34:841–855
- Shapiro AM, Lakey JR. Future trends in islet cell transplantation. *Diabetes Technol Ther* 2000;2:449–452
- Yamada M, Johannesson B, Sagi I, et al. Human oocytes reprogram adult somatic nuclei of a type 1 diabetic to diploid pluripotent stem cells. *Nature* 2014;510:533–536
- Maehr R, Chen S, Snitow M, et al. Generation of pluripotent stem cells from patients with type 1 diabetes. *Proc Natl Acad Sci USA* 2009;106:15768–15773
- Johannesson B, Sagi I, Gore A, et al. Comparable frequencies of coding mutations and loss of imprinting in human pluripotent cells derived by nuclear transfer and defined factors. *Cell Stem Cell* 2014;15:634–642
- Wakayama S, Kohda T, Obokata H, et al. Successful serial recloning in the mouse over multiple generations. *Cell Stem Cell* 2013;12:293–297
- Gao S, Zheng C, Chang G, et al. Unique features of mutations revealed by sequentially reprogrammed induced pluripotent stem cells. *Nat Commun* 2015;6:6318
- Yamada M, Byrne J, and Egli D. From cloned frogs to patient matched stem cells: induced pluripotency or somatic cell nuclear transfer? *Curr Opin Genet Dev* 2015;34:29–34
- Micallef SJ, Li X, Schiesser JV, et al. INS(GFP/w) human embryonic stem cells facilitate isolation of in vitro derived insulin-producing cells. *Diabetologia* 2012;55:694–706
- Goulburn AL, Alden D, Davis RP, et al. A targeted NKX2.1 human embryonic stem cell reporter line enables identification of human basal forebrain derivatives. *Stem Cells* 2011;29:462–473
- Adewola AF, Lee D, Harvat T, et al. Microfluidic perfusion and imaging device for multi-parametric islet function assessment. *Biomed Microdevices* 2010;12:409–417
- Mohammed JS, Wang Y, Harvat TA, Oberholzer J, Eddington DT. Microfluidic device for multimodal characterization of pancreatic islets. *Lab Chip* 2009;9:97–106
- Kayton NS, Poffenberger G, Henske J, et al. Human islet preparations distributed for research exhibit a variety of insulin-secretory profiles. *Am J Physiol Endocrinol Metab* 2015;308:E592–E602
- Kroon E, Martinson LA, Kadoya K, et al. Pancreatic endoderm derived from human embryonic stem cells generates glucose-responsive insulin-secreting cells in vivo. *Nat Biotechnol* 2008;26:443–452
- Sui L, Mfopou JK, Chen B, Sermon K, Bouwens L. Transplantation of human embryonic stem cell-derived pancreatic endoderm reveals a site-specific survival, growth, and differentiation. *Cell Transplant* 2013;22:821–830
- Pagliuca FW, Millman JR, Gürtler M, et al. Generation of functional human pancreatic β cells in vitro. *Cell* 2014;159:428–439
- Rezania A, Bruin JE, Arora P, et al. Reversal of diabetes with insulin-producing cells derived in vitro from human pluripotent stem cells. *Nat Biotechnol* 2014;32:1121–1133
- Sander M, Sussel L, Connors J, et al. Homeobox gene *Nkx6.1* lies downstream of *Nkx2.2* in the major pathway of beta-cell formation in the pancreas. *Development* 2000;127:5533–5540
- D'Amour KA, Bang AG, Eliazar S, et al. Production of pancreatic hormone-expressing endocrine cells from human embryonic stem cells. *Nat Biotechnol* 2006;24:1392–1401
- Nostro MC, Sarangi F, Yang C, et al. Efficient generation of NKX6-1+ pancreatic progenitors from multiple human pluripotent stem cell lines. *Stem Cell Rep* 2015;4:591–604
- Sui L, Geens M, Sermon K, Bouwens L, Mfopou JK. Role of BMP signaling in pancreatic progenitor differentiation from human embryonic stem cells. *Stem Cell Rev* 2013;9:569–577
- Brissova M, Fowler MJ, Nicholson WE, et al. Assessment of human pancreatic islet architecture and composition by laser scanning confocal microscopy. *J Histochem Cytochem* 2005;53:1087–1097
- Butler AE, Robertson RP, Hernandez R, Matveyenko AV, Gurlo T, Butler PC. Beta cell nuclear musculoaponeurotic fibrosarcoma oncogene family A (*MafA*) is deficient in type 2 diabetes. *Diabetologia* 2012;55:2985–2988
- Kind A, Colman A. Therapeutic cloning: needs and prospects. *Semin Cell Dev Biol* 1999;10:279–286
- Lanza RP, Cibelli JB, West MD. Human therapeutic cloning. *Nat Med* 1999;5:975–977
- Kassem SA, Ariel I, Thornton PS, Scheimberg I, Glaser B. Beta-cell proliferation and apoptosis in the developing normal human pancreas and in hyperinsulinism of infancy. *Diabetes* 2000;49:1325–1333
- Hayek A, Beattie GM. Experimental transplantation of human fetal and adult pancreatic islets. *J Clin Endocrinol Metab* 1997;82:2471–2475
- Aynsley-Green A, Bloom SR, Williamson DH, Turner RC. Endocrine and metabolic response in the human newborn to first feed of breast milk. *Arch Dis Child* 1977;52:291–295
- Mitanchek-Mokhtari D, Lahlou N, Kieffer F, Magny JF, Roger M, Voyer M. Both relative insulin resistance and defective islet beta-cell processing of proinsulin are responsible for transient hyperglycemia in extremely preterm infants. *Pediatrics* 2004;113:537–541
- Millman JR, Xie C, Van Dervort A, Gürtler M, Pagliuca FW, and Melton DA. Generation of stem cell-derived beta-cells from patients with type 1 diabetes. *Nat Commun* 2016;7:11463
- Nishizawa M, Chonabayashi K, Nomura M, et al. Epigenetic variation between human induced pluripotent stem cell lines is an indicator of differentiation capacity. *Cell Stem Cell* 2016;19:341–354
- Chan XY, Black R, Dickerman K, et al. Three-dimensional vascular network assembly from diabetic patient-derived induced pluripotent stem cells. *Arterioscler Thromb Vasc Biol* 2015;35:2677–2685
- Kalscheuer H, Danzi N, Onoe T, et al. A model for personalized in vivo analysis of human immune responsiveness. *Sci Transl Med* 2012;4:125ra30